The Cryosphere Discuss., 8, 1095–1110, 2014
www.the-cryosphere-discuss.net/8/1095/2014/
doi:10.5194/tcd-8-1095-2014

The Cryosphere
Discussions
Open Access

The impact of ice layers on gas transport through firn

K. Keegan, M. R. Albert, and I. Baker

Thayer School of Engineering, Dartmouth College, Hanover, NH, USA

Received: 13 January 2014 – Accepted: 30 January 2014 – Published: 10 February 2014

Correspondence to: K. Keegan (kaitlin.m.keegan.th@dartmouth.edu)

Published by Copernicus Publications on behalf of the European Geosciences Union.

Abstract

Typically, gas transport through firn is modeled in the context of an idealized firn column. However, in natural firn, imperfections are present which may alter transport dynamics in ways that may reduce the accuracy of climate records. For example, ice layers have been found in several firn cores collected in the polar regions. Here, we examined the effects of two ice layers found in a NEEM, Greenland firn core on gas transport through the firn. Both ice layers were somewhat permeable. However, only the shallower ice layer was significantly less permeable than the surrounding firn and is therefore likely to retard gas transport. Large closed bubbles were found in one ice layer, which would contain older atmospheric samples than expected. Theses bubbles are likely to significantly bias age estimates. Conversely, the permeability and thickness of ice layers at NEEM suggest that they will not significantly bias the expected firn air concentration profiles at the present spatial resolution at which these data are collected. Therefore, ice layers do not need to be accounted for in gas transport models at NEEM. However, the microstructure of these ice layers indicates that larger melting events could significantly bias ice core records.

1 Introduction

In the coldest regions of an ice sheet, glacial ice is formed from the densification of snow due to the overburden pressure of successive precipitation events. This transition from snow to glacial ice occurs over hundreds of years, and creates a region at the top of the ice sheet known as the firn column. The firn column thickness is typically 40–120 m in depth, depending on the site conditions, and contains interconnected pore space within the layers of firn. The interconnected pore space allows gases from the overlying atmosphere to diffuse to the bottom of the firn column where they are trapped in bubbles as the deepest firn layers transition into glacial ice. The firn column creates an inherent age difference (Δ age) between the ice and the bubbles it traps, which is an important parameter for interpreting ice core records (Schwander and Stauffer, 1984).

Melt rarely occurs in the dry snow regions of an ice sheet, making those areas valuable sites for drilling ice cores to retrieve long term climate records (Benson, 1962). However, melt events do occur occasionally in the dry snow region, such as the widespread melting events of the Greenland ice sheet in 2012 (Nghiem et al., 2012; Bennartz et al., 2013) and 1889 (Keegan et al., 2014). The melt water from these events refreezes into ice layers within the snowpack near the surface of the ice sheet, and locally disrupts the interconnected pore space. The rate of gas transport through the firn column is modeled assuming a continuously connected pore space through the firn column until the lock-in depth (Buizert et al., 2012). Therefore, the models do not account for any pore space disruption due to ice layers formed from melt. At the Law Dome site, an ice layer did require incorporating a low permeability section of the firn column to the modeled gas diffusivity in order to reconcile the modeled diffusivity profile with the discrete firn gas samples (Trudinger et al., 1997). However, it is unclear when ice layers need to be accounted for when modeling gas transport through the firn.

In this study, we examine the permeability of ice layers found in a firn core retrieved from NEEM, Greenland in an effort to understand the impact that ice layers have on gas transport through the firn column. We also investigate microstructural properties of these ice layers, and discuss the effect of air bubbles included in the layers during the refreezing process. Lastly, we discuss ways to address ice layers when modeling gas transport through firn.

2 Methods

2.1 NEEM firn core

The NEEM 2009 S2 shallow firn core was drilled in July 2009 from a firn-air sampling site approximately 1 km from the main drilling site at NEEM, Greenland. The core was drilled to a depth of 76 m and shipped back to the laboratory for analysis. In the cold laboratory, we documented the stratigraphy and qualitatively characterized the grain size with 1 mm depth resolution for the entire length of the core. We then cut the core into subsections of 5–10 cm in height, retaining samples of homogeneous layering as often as possible. The physical dimensions of each core piece were measured using calipers and a millimeter-scale rule, and any imperfections in the sample were noted. The mass of each core piece was measured using a calibrated balance. We calculated the density for each core subsection from the measured height, diameter, and mass for each.

2.2 Permeability

Permeability is a measure of a porous media's ability to transport gases through its interconnected pore space. Permeability is defined from Darcy's Law (Eq. 1) as the proportionality constant, k, which relates the pressure gradient to the flow rate of air through the sample:

$$v = \frac{k}{\mu}\frac{\mathrm{d}P}{\mathrm{d}z} \tag{1}$$

where v is the air flow velocity, μ is the fluid viscosity, P is the pressure, and z is the height of the sample. In deep firn, the permeability is linearly related to the gas diffusivity (Adolph and Albert, 2013).

To determine the permeability of our firn core, we measured the pressure drop over the height of each homogenous subsection of firn while varying the flow rate of air through the samples using a custom permeameter previously developed (Albert et al., 2000). The measured geometrical dimensions, flow rate, pressure drop, air temperature, and barometric pressure were then used to calculate the permeability from Darcy's law. Measurements that fell outside of the linear flow range were not used. On average, eight to ten permeability measurements were made on each sample using different flow rates. The difference in permeability values for replicate measurements is within 3 % per sample, and within 6 % for standard glass beads. It was found that the permeability of a firn depth varied by as much as 10 % due to the spatial heterogeneity within a given layer at a Greenland field site (Albert et al., 2000).

2.3 X-ray micro-computed tomography

We examined the three-dimensional structure of the firn and ice layers in the core using x-ray micro-computed tomography (micro-CT). Using a Skyscan 1172 micro-CT housed within in a cold room, we scanned 10 mm × 10 mm × 15 mm samples containing the ice layers. We used the software programs NRECON™, CTAn™, and CTVol™ to reconstruct the three-dimensional images and calculated microstructural properties of the ice layer samples. The microstructural properties we examined were closed porosity, number of closed pores, and volume of closed pores.

3 Results and discussion

3.1 NEEM ice layers

We identified two ice layers in the NEEM firn core at depths of 27.3 m and 44.3 m depth (Fig. 1). These ice layers are 1–2 cm in thickness and exhibit multiple ice horizons in close proximity at both depths. The structure of the ice layers is distinctly different from that of wind crusts, which are mono-grain layers of wind-packed snow that are on the order of millimeters in thickness and are commonly found in firn stratigraphy (Alley, 1988). The thickness of the NEEM ice layers indicates that they were formed from the refreezing of melt water within the near-surface snowpack at this site. The presence of multiple ice horizons at both ice layer depths is an indication that there was sufficient melting, which caused percolation of melt water deeper into the firn. In investigations of the nature of the percolation of the 2012 event at Summit, it has been found that the infiltration of melt fingers into the underlying firn terminated in small refrozen melt pools approximately 20 cm deeper than the original melt horizon (Adolph et al., 2014). The depth of the multiple underlying melt layers at a given site will depend on the nature of the melt event, the temperature of the firn, and the amount of liquid water available for percolation.

Using a depth-age scale determined through chemistry (J. McConnell, personal communication, 2013), the shallower ice layer (Ice Layer 1) was dated to 1941 AD and the deeper ice layer (Ice Layer 2) was dated to 1888 AD. Interestingly, it was found that Ice Layer 2 was formed from the last widespread surface-melting event on the Greenland ice sheet in 1889 (Keegan et al., 2014), which produced ice layers that are clearly visible in firn cores that have been retrieved from many sites across Greenland. Ice Layer 1 appears to have been formed from a local melting event at NEEM, as it has not been identified in other firn cores in Greenland.

The firn density profiles near each ice layer are shown in Fig. 2. The average density of the firn from 23.5–28.5 m was 0.616 $\mathrm{g\,cm^{-3}}$, with a standard deviation of 0.015 $\mathrm{g\,cm^{-3}}$. The density of the core sample containing Ice Layer 1 was 0.648 $\mathrm{g\,cm^{-3}}$, which is outside the normal firn layer density variation as it is greater than two standard deviations from the mean at that depth. The average density of the firn from 40.5–46.5 m was 0.713 $\mathrm{g\,cm^{-3}}$, with a standard deviation of 0.017 $\mathrm{g\,cm^{-3}}$. The density of the core sample containing Ice Layer 2 was 0.719 $\mathrm{g\,cm^{-3}}$, and is not statistically different than the firn layers around it because of the extent of firn densification at this depth.

3.2 Permeability

The permeability profile of the firn near each ice layer is shown in Fig. 3. The average permeability from 23.5–28.5 m was $10.98 \times 10^{-10}\ \mathrm{m^2}$, with a standard deviation of $2.84 \times$

10^{-10} m^2. The permeability of the core sample containing Ice layer 1 was 3.0×10^{-10} m^2, which is significantly lower than the surrounding firn layers. A permeability value below 0.1×10^{-10} m^2 is considered to be impermeable due to the measurement capabilities of the permeameter. Therefore, our results indicate that Ice Layer 1 is not impermeable despite having a permeability that is lower than the surrounding firn.

The average permeability from 40.5–46.5 m was 4.05×10^{-10} m^2, with a standard deviation of 1.41×10^{-10} m^2. The permeability of the core sample containing Ice layer 2 was 4.0×10^{-10} m^2. Since the permeability of Ice layer 2 is within one standard deviation of the mean, it is not significantly different than the surrounding firn at this depth. At these depths the firn layers are more dense and therefore less permeable, causing the permeability of the ice layer and firn to be similar.

Both NEEM firn ice layers are permeable, and hence will permit gas transport. Interestingly, the permeability of these ice layers in the polar firn at NEEM are nearly the same as the permeability of ice layers found in seasonal snow (Albert and Perron, 2000). However, the polar firn surrounding Ice Layer 1 had higher permeabilities ranging from 5–18 × 10^{-10} m^2 compared to the seasonal snow. If the ice layer extends laterally for great distances, such a permeable ice layer would not cause a disruption in the gas concentration profile under steady state conditions at this depth. However, for gases that experience time-varying effects within the firn column, a laterally-extensive ice layer at 27 m may be expected to cause some variation within the concentration profile even though it does not totally impede gas diffusion. In contrast, the permeability of Ice Layer 2 at 44 m depth is very similar in magnitude to the permeability of the surrounding firn, and thus would likely not cause a disruption in either steady state or time-varying diffusion concentration profiles. Our findings of permeable ice layers are consistent with the absence of firn-air gas diffusion disruption in the diffusive zone of the NEEM firn column (Buizert et al., 2012).

3.3 Microstructure of ice layers

To investigate the microstructure of these permeable ice layers, we conducted three-dimensional imaging of sections of each ice layer with the micro-CT. The reconstructed images of the ice and pore phases of both ice layers are shown in Fig. 4. The ice phase images (Fig. 4a and b) show a continuous ice layer with few pores in the both samples, indicating the ice horizon seen visually. The pore phase image of Ice Layer 1 (Fig. 4c) shows one large horizontally connected pore running through the ice layer, which indicates that there are large pores directing gas transport through the ice layer. The pore phase image of Ice Layer 2 (Fig. 4d) shows a few large and many small air bubbles that were trapped in the refreezing process that layer. The bubbles within the ice layers closed when they were near the surface, and therefore contain atmospheric samples that are much older than bubbles formed normally at the bottom of the firn column. If bubbles occluded within ice layers are large enough, they could bias the age of gas records to be older than expected at that depth.

To investigate the effect that these bubbles have on the NEEM firn-air record the average bubble size, maximum bubble volume, and total bubble volumes were calculated from the reconstructed micro-CT images (Table 1). Ice layer 1 contained only small bubbles, which caused 0.2 % of the porosity to be closed on average, which would not contribute significantly to the incorporated gas record. Ice Layer 2 contained bubbles with an average size of 0.75 mm^3, with the largest bubble having a closed volume of 2.6 mm^3. At this depth, the largest bubbles represent 6 % of the porosity.

Bubble formation above the lock-in zone of a firn column can be studied by examining the gravitational enrichment of δ^{15}N in the firn. Any bubbles closed at the surface would contain approximately 0 ‰ δ^{15}N, because the near surface firn is well mixed with the atmosphere. At NEEM, the firn air δ^{15}N content is approximately 0.28 ‰ at the bottom of the firn column (Buizert et al., 2012). In order to detect a difference in age between the air inside the bubbles and the air within the open porosity, there must be a difference of at least 5.4 per meg δ^{15}N (Battle et al., 2011). Assuming a concentration of 0.0001 ‰

of δ^{15}N within the closed ice layer air bubbles, it will require approximately 3.5 % of the porosity to be closed into bubbles. Therefore, it is likely that the air bubbles within Ice Layer 2 would bias the age of that firn layer towards older estimates. Since melt events give rise to ice layers near the surface of the firn column, they have the ability to affect the ice core gas records more than anomalously occluded bubbles deeper in the firn. However, ice layers found in the dry snow region of Greenland are on the order of 1 cm in thickness. Since the current continuous flow analysis technology allows 10 mm resolution of ice core strata, a single ice layer would not significantly bias the ice core records (Bigler et al., 2011). If melt events created thicker ice layers than those displayed in the NEEM 2009 firn core, larger trapped bubbles could bias the ice core records more significantly.

4 Conclusions

Both ice layers in the NEEM 2009 firn core were permeable. However, only the shallower layer was significantly less permeable than the surrounding firn. Nevertheless, ice layers ultimately should not affect the steady-state gas concentration profile in the firn. In shallow firn, however, ice layers may affect the concentration profile of fast-diffusing species in non-steady-state diffusion conditions. In both deep and shallow ice layers, air bubbles were trapped during the refreezing process of the surface melt. These air bubbles probably contain atmospheric samples that are much older than expected for the surrounding firn, and significantly biasing the ice core record at that depth. Nevertheless, these ice layers were relatively thin and are therefore not expected to significantly alter the gas record because of the spatial resolution of current gas records. Taken as a whole, our results suggest that the effects of ice layers do not need to be accounted for when modeling firn gas transport at NEEM, though the effects of ice layer microstructure may be significant at other sites.

Acknowledgements. We thank Z. Courville and the NEEM 2009 firn-air campaign team for assistance in collecting the NEEM 2009-S2 core. Collection and analysis of the core was supported by NSF-ARC 0806339. This work also was supported by NSF-PIRE 0968391 and the Dartmouth College IGERT NSF-DGE 0801490 grants. The authors would also like to acknowledge M. Logan, and M. Battle for their helpful discussions. NEEM is directed and organized by the Center of Ice and Climate at the Niels Bohr Institute and US NSF, Office of Polar Programs. It is supported by funding agencies and institutions in Belgium (FNRS-CFB and FWO), Canada (NRCan/GSC), China (CAS), Denmark (FIST), France (IPEV, CNRS/INSU, CEA and ANR), Germany (AWI), Iceland (RannIs), Japan (NIPR), Korea (KOPRI), the Netherlands (NWO/ALW), Sweden (VR), Switzerland (SNF), UK (NERC) and the USA (US NSF, Office of Polar Programs).

References

Adolph, A. C. and Albert, M. R.: The physical basis for gas transport through polar firn: a case study at Summit, Greenland, The Cryosphere Discuss., 7, 2455–2487, doi:10.5194/tcd-7-2455-2013, 2013.

Adolph, A. C. and Albert, M. R.: Radar investigations of melt percolation from the 2012 melt event at Summit, Greenland, in review, 2014.

Albert, M. R. and Perron, F. E.: Ice layer and surface crust permeability in a seasonal snow pack, Hydrol. Process., 14, 3207–3214, 2000.

Albert, M. R., Shultz, E. F., and Perron, F. E.: Snow and firn permeability at Siple Dome, Antarctica, Ann. Glaciol., 31, 353–356, 2000.

Alley, R. B.: Concerning the deposition and diagenesis of strata in polar firn, J. Glaciol., 34, 283–290, 1988.

Battle, M. O., Severinghaus, J. P., Sofen, E. D., Plotkin, D., Orsi, A. J., Aydin, M., Montzka, S. A., Sowers, T., and Tans, P. P.: Controls on the movement and composition of firn air at the West Antarctic Ice Sheet Divide, Atmos. Chem. Phys., 11, 11007–11021, doi:10.5194/acp-11-11007-2011, 2011.

Bennartz, R., Shupe, M. D., Turner, D. D., Walden, V. P., Steffen, K., Cox, C. J., Kulie, M. S., Miller, N. B., and Pettersen, C.: July 2012 Greenland melt extent enhanced by low-level liquid clouds, Nature, 496, 83–86, 2013.

Benson, C. S.: Stratigraphic studies in the snow and firn of the Greenland ice sheet, US Army Corps of Engineers Special Report, SIPRE Res. Rep., 70, 24–25, 1962.

Bigler, M., Svensson, A., Kettner, E., Vallelonga, P., Nielsen, M. E., and Steffensen, J. P.: Optimization of high-resolution continuous flow analysis for transient climate signals in ice cores, Environ. Sci. Technol., 45, 4483–4489, 2011.

Buizert, C., Martinerie, P., Petrenko, V. V., Severinghaus, J. P., Trudinger, C. M., Witrant, E., Rosen, J. L., Orsi, A. J., Rubino, M., Etheridge, D. M., Steele, L. P., Hogan, C., Laube, J. C., Sturges, W. T., Levchenko, V. A., Smith, A. M., Levin, I., Conway, T. J., Dlugokencky, E. J., Lang, P. M., Kawamura, K., Jenk, T. M., White, J. W. C., Sowers, T., Schwander, J., and Blunier, T.: Gas transport in firn: multiple-tracer characterisation and model intercomparison for NEEM, Northern Greenland, Atmos. Chem. Phys., 12, 4259–4277, doi:10.5194/acp-12-4259-2012, 2012.

Keegan, K. M., Albert, M. R., McConnell, J. R., and Baker, I.: Climate change and forest fires synergistically drive widespread melt of the Greenland Ice Sheet, in review, 2014.

Nghiem, S. V., Hall, D. K., Mote, T. L., Tedesco, M., Albert, M. R., Keegan, K., Shuman, C. A., DiGirolamo, N. E., and Neumann, G.: The extreme melt across the Greenland ice sheet in 2012, Geophys. Res. Lett., 39, L20502, doi:10.1029/2012GL053611, 2012.

Schwander, J. and Stauffer, B.: Age difference between polar ice and the air trapped in its bubbles, Nature, 311, 45–47, 1984.

Trudinger, C. M., Enting, I. G., Etheridge, D. M., Francey, R. J., Levchenko, V. A., Steele, L. P., Raynaud, D., and Arnaud, L.: Modeling air movement and bubble trapping in firn, J. Geophys. Res., 102, 6747–6763, 1997.

Table 1. Microstructural parameters of ice layer bubbles.

Sample	Avg. Bubble Volume (mm^3)	Max. Bubble Volume (mm^3)	Total Bubble Volume (%)
Ice Layer 1	0.03	0.07	0.2
Ice Layer 2	0.20	2.62	6.0

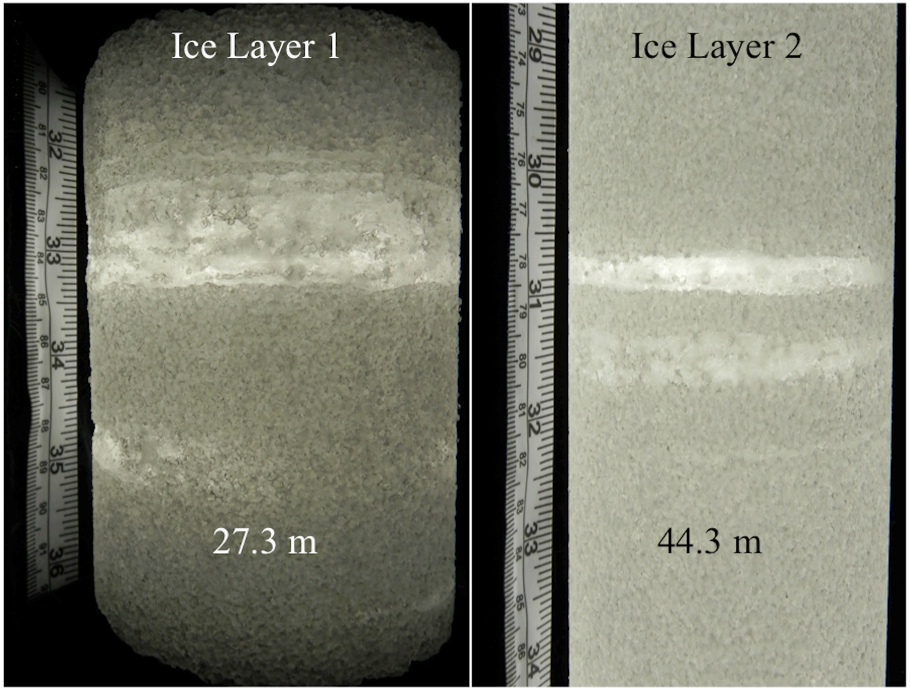

Fig. 1. The two ice layers in the 2009 NEEM firn core; (left) Ice Layer 1 located at 27.3 m depth, and (right) Ice Layer 2 located at 44.3 m depth.

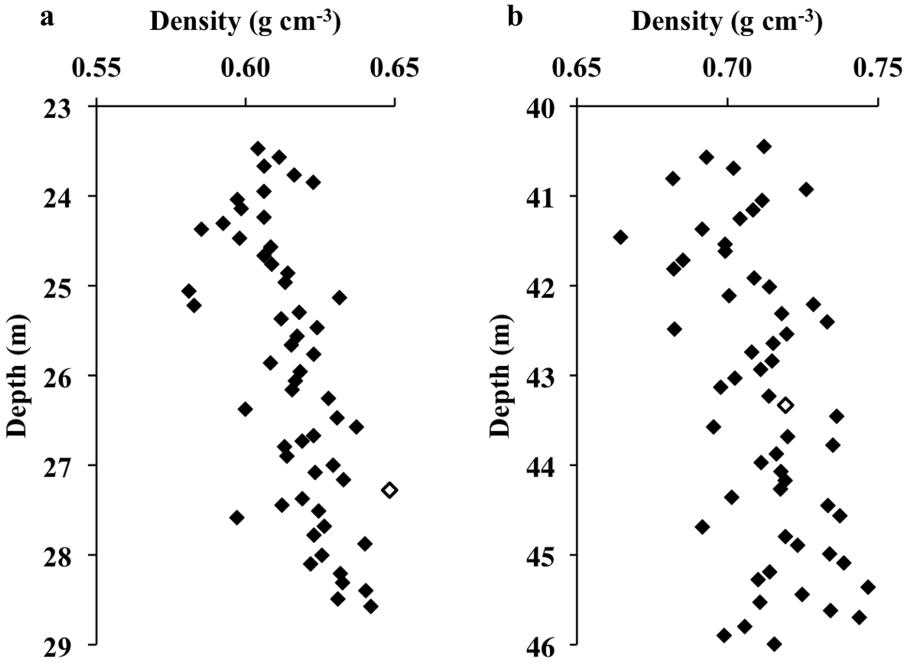

Fig. 2. The density profiles near **(a)** Ice Layer 1, and **(b)** Ice Layer 2, where the closed diamonds indicate normal firn core samples and the open diamonds indicate the core sample containing the ice layer.

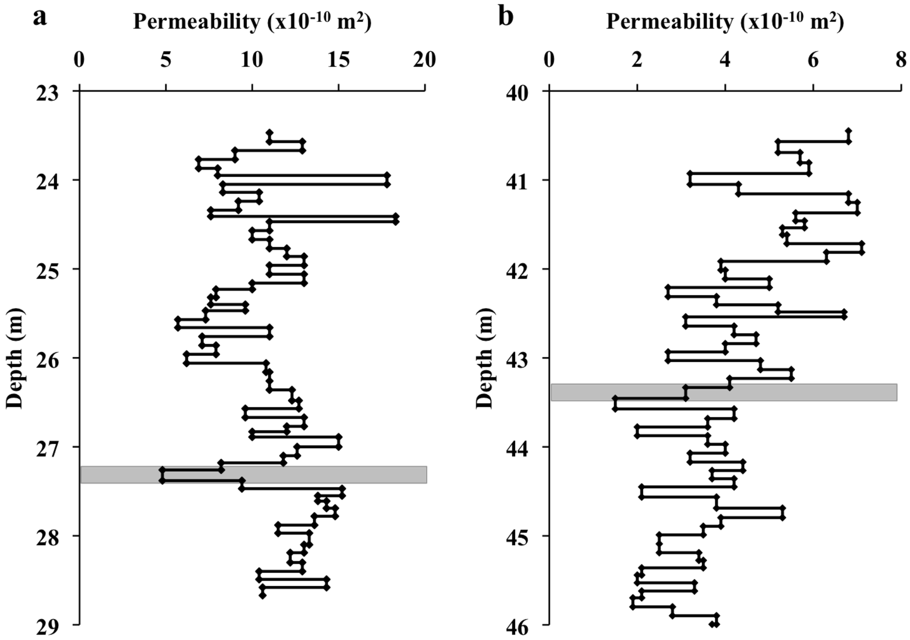

Fig. 3. The permeability profiles from the 2009 NEEM firn core, near **(a)** Ice layer 1, **(b)** Ice layer 2. Grey bars indicate ice layer samples.

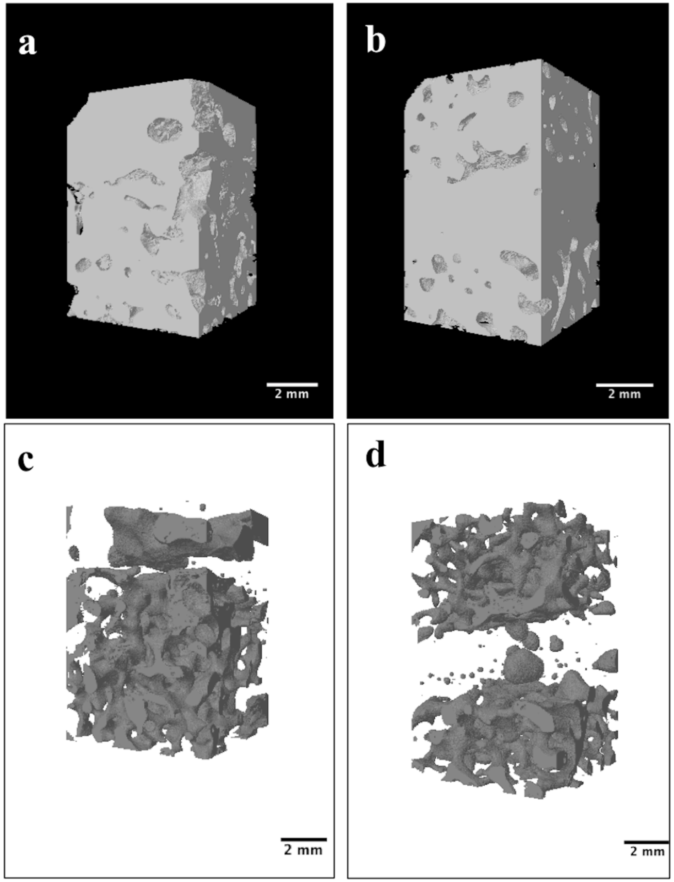

Fig. 4. Reconstructed three-dimensional images of the ice phase of **(a)** Ice Layer 1 and **(b)** Ice Layer 2, and the pore phase of **(c)** Ice Layer 1 and **(d)** Ice Layer 2.